SYNTHESIS OF GRAPHENE/$CuGaO_2$ AEROGELS FOR ADVANCED ELECTRODES

Cristina Mosoarca[1], **Daniel Ursu**[1], **Terezia Nyari**[1], **Petrica Linul**[1,2], **Iuliana Serbachievici**[1], **Bogdan Taranu**[1], **Radu Banica**[1]

[1]*National Institute for Research and Development in Electrochemistry and Condensed Matter, Dr. A. Paunescu Podeanu, no. 144, Timisoara, Romania*
[2]*Politehnica University Timisoara, Piata Victoriei, no. 2, Timisoara, Romania*
e-mail: radu.banica@yahoo.com

Abstract

Inorganic aerogels [1] are most often produced from silica, undergoing multiple phases of cooling and heating under high pressure (supercritical drying) or vacuum (lyophilization). Nowadays, low-cost organic aerogels such as graphene/metal oxide hydrogels are widely used in various applications (supercapacitors, oil absorption etc.) and fields like electronics, material science and aerospace engineering [2,3]. These carbon-based nanomaterials, having a nonpolar carbon structure, are useful especially for their essential hydrophobic properties [4], ultralow density, high surface area and high conductivity. Our previous work [5,6] included studies upon *p*-$CuGaO_2$ dye-sensitized solar cells which revealed excellent optical transparency of $CuGaO_2$. Also, $CuGaO_2$ can be used in photocatalysis for the oxidation of hydrogen sulfide, while graphene can conduct the electrons generated in the conduction band of the semiconductor to the counter-electrode closing the electrical circuit. Hybrid materials like $CuGaO_2$/graphene aerogels could be efficient for dye-sensitized solar cells and advanced electrodes fabrication.

Experimental

The precursor sample (P1) is a mixture of graphene oxide prepared using a modified Hummers method (conc. 0.9 mg/ml) and graphene Quattro-Type (conc. 0.05 mg/l) purchased from NanoIntegris. By centrifugation and water redispersion, the concentration of graphene increased to 0.75 mg/ml.

Further, the suspension was subjected to freeze drying and thermal treatment in a GSL-1500X Vacuum furnace (MIT Corporation) at a pressure < 1 Torr and a temperature rise rate of -4°C/minute resulting in P1T2 (Fig. 1A) and P1T3 samples.

$CuGaO_2$ was obtained under hydrothermal conditions at 250ºC, using metal nitrates as precursors. X-Ray powder diffraction patterns of $CuGaO_2$ were obtained using an X'Pert PRO MPD diffractometer.

$CuGaO_2$ was added to P1 aqueous solution, following the protocol described above, resulting in aerogel samples S1 and S2 (Fig. 1B). Samples S1 and S2 were characterized by Scanning Electron Microscopy (SEM).

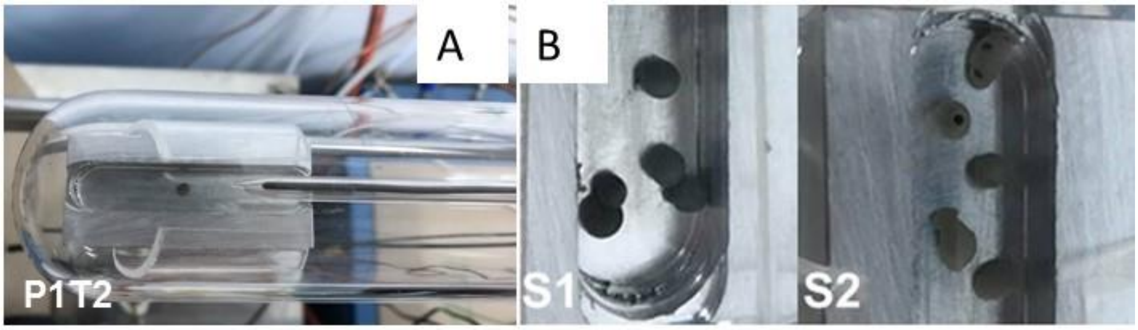

Figure 1. Photograph of (A) P1T2 aerogel sample (B) S1 and S2 aerogel samples

Results and discussion

Sample composition and processing conditions are presented in Table 1.

Sample name	**$CuGaO_2$ %**	**Treatment temperature °C**
P1T2	**0**	**240**
P1T3	**0**	**300**
S1	**1**	**300**
S2	**4**	**300**

Table 1. Experimental conditions for thermal treatment and $CuGaO_2$ content corresponding to P1T2, P1T3, S1 and S2 samples

The sample P1T3 (Fig. 1A), resulting from the 300°C thermal treatment (Table 1), has an average pore size higher than sample P1T2 obtained at 240°C. This phenomenon is due to the lower density of hydrophilic groups as G-COOH, G-OH, G-CO, attached on the graphene sheets**.** A high density of functional groups leads to the adsorption of a higher quantity of atmospheric water which, in turn, leads to the loss of structural integrity and partial collapse of structures, manifested by the pore dimension decrease.

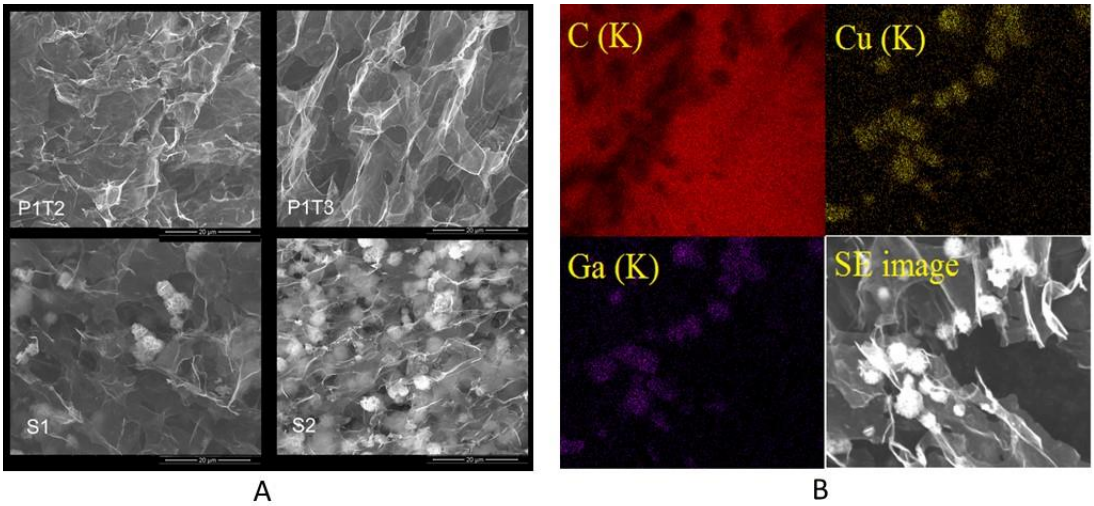

Figure 2. Graphene and CuGaO2/graphene aerogels – (A) SEM images of P1T2, P1T3, S1 and S2 samples; (B) EDS elemental composition maps of S1 sample.

In case of S1 and S2 aerogel samples, we can see that the $CuGaO_2$ "flower shape" superstructures are uniformly distributed in the volume of the graphene aerogel (Fig. 2A and 2B). Due to the use of the graphite oxide and reduced graphene mixture, the S1 and S2 aerogels have both a high polar molecule absorption capacity due to the functional groups attached to the graphene oxide and, also, a high electrical conductivity due to the reduced graphene.

EDS maps (Fig. 2B) of S1 sample confirmed the homogenous distribution of Cu and Ga, which confirms the pure phase $CuGaO_2$ delafossite (Fig. 3) and the relative homogenous dispersion of the inorganic compound in aerogel. The use of hybrid materials like $CuGaO_2$/graphene type aerogels, for dye-sensitized solar cells, electrochemical sensors and advanced electrodes will be the topic of further studies.

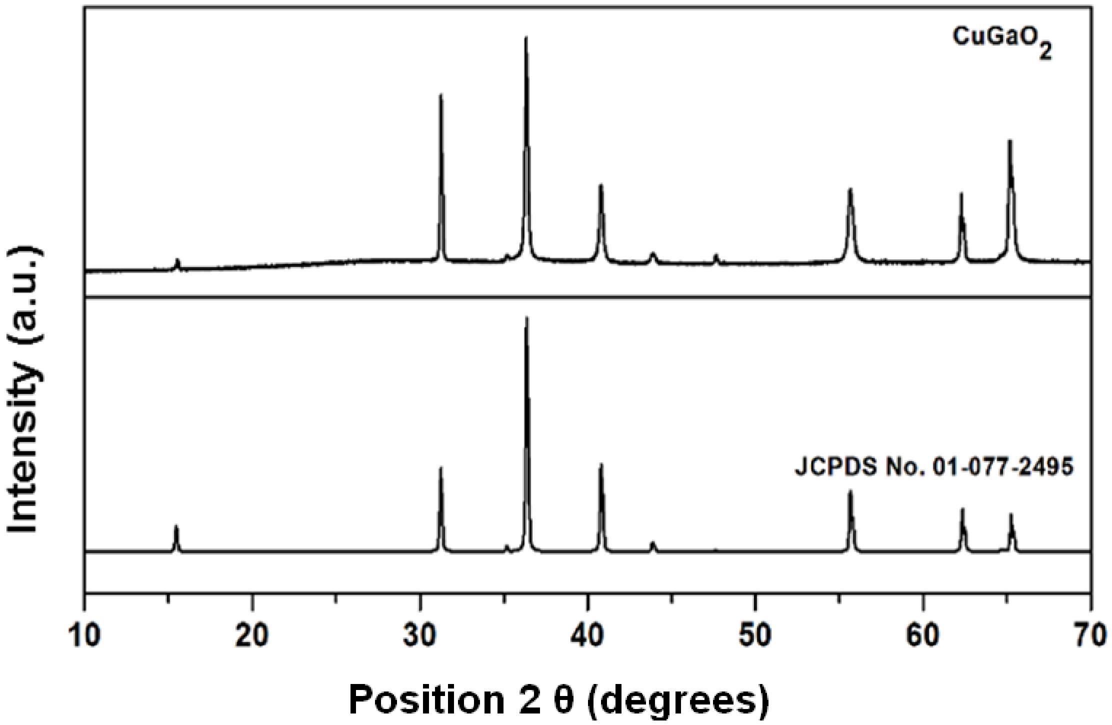

Figure 3. X-ray diffraction pattern of $CuGaO_2$

TEM image (Fig. 4A) suggests that *p*-$CuGaO_2$ semiconductor is exhibiting flat platelets. These semiconductor sheets are forming spherical superstructures coated by graphene within the aerogel. Therefore, the electrical contact between the graphene layer and the semiconductor nanoparticle is "point shaped" with reduced surface area. Further studies are required for increasing the contact surface between the semiconductor and graphene sheets.

The band gap energy value of the semiconductor (Eg) was determined from the UV-Vis diffuse reflectance spectra (Fig. 4B). Sample reflectance was transformed into absorbance using Kubelka-Munk (K-M) function. Due to the fact that $CuGaO_2$ has a direct inter-band transition, the Eg value was determined by extrapolating the linear part of $(K\text{-}M{*}E)^2 = f(E)$, where K-M is the absorbance and E the reflected energy radiation (eV) [7].

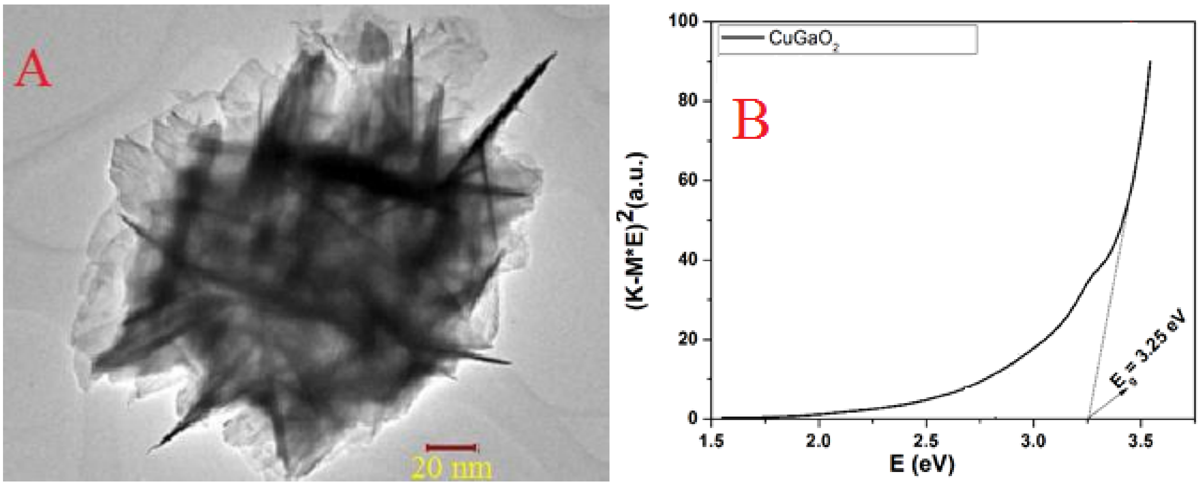

Figure 4. TEM of pure CuGaO$_2$ material (A) and Eg determination (B)

Conclusions

Graphene and graphene/CuGaO$_2$ based aerogels, with various possible nanotechnology applications, were synthetized by lyophilization followed by thermal treatment in vacuum. During the thermal treatment, the graphene oxide from precursors is partially reduced; some hydrophilic bonds are lost by condensation and decarboxylation reactions, leading to aerogel pore size change after water adsorption. An aerogel with a homogenous distribution of the semiconductor within it was obtained by mixing P1 aqueous suspension containing graphene oxide and reduced graphene with the CuGaO$_2$ compound, before freezing.

Acknowledgements

This work was supported by a grant of the Romanian Ministry of Research and Innovation, CCCDI-UEFISCDI, project number PN-III-P1-1.2-PCCDI-2017-0619/Contract 42/2018 “Nanostructured carbon materials for advanced industrial applications”, within PNCDI III national research program.

References

[1] S.S. Kistler, Nature, 127 (1931) 741.
[2] G. Gorgolis, C. Galiotis, 2D Materials, 7 (2017) 032001.
[3] G Tang, Z.G Jiang, X. Li, H.B. Zhang, A. Dasari, Z.Z Yu, Carbon, 77 (2014) 592-599.
[4] Y. Lin, G.J. Ehlert, C. Bukowsky, H.A. Sodano, Appl. Mater. Interfaces, 3 (2011) 2200–2203.
[5] D. Ursu, M. Miclau, R. Banica, N. Vaszilcsin, Mat. Lett. 143 (2015) 91-93.
[6] C. Zamfirescu, I. Dincer, G.F. Naterer, R. Banica, Chem. Eng. Sci. 97 (2013) 235-255.
[7] R. Banica, T. Nyari, V. Sasca, Int. J. Hydrogen Energ. 37 (2012) 16489 – 16497.